DETERMINATION OF INDIVIDUAL DROPLET CHARGE IN ELECTROSPRAYS FROM PDPA MEASUREMENTS

T. Gemci, R. Hitron, and N. Chigier
Email: chigier@andrew.cmu.edu
Spray Systems Technology Center, Mechanical Engineering Dept.
Carnegie Mellon University, Pittsburgh, PA 15213

Abstract
Determination of the droplet specific charge (charge-to-mass ratio) for a cone-jet is described based on Phase Doppler Interferometry measurements of droplet size and velocities. In an electrospray process theoretical limits on the charge of a droplet are imposed by the Rayleigh and Paschen equations. Electrostatically charged sprays have a wide variety of applications such as automobile painting, micro electronic, ultra thin film coating, medical, and inhalation therapy sprays. The influence of applied voltage on the drop size distribution is dominant in many applications.

Introduction

The objective of many spraying applications is to distribute liquid onto a selected target in a controlled and predetermined way. Electrostatic forces can be used to deflect charged drop trajectories, so that drop deposition onto a target can be controlled. For accurate targeting, not only is it essential for drops to be charged but the magnitude of the charge must be controlled. In some situations, where targeting requirements are precise, as for example with ink-jet printing, drops are equi-sized and charge levels may be controlled with great accuracy. Spray painting is another controlled situation in which electrostatic spraying of earthed objects of well-defined geometries is used. Spray distance, angle, and charge levels can be adjusted for optimum coating.

Droplet charge density or charge-to-mass ratio is the basic parameter that affects the electrohydrodynamic atomization characteristics. The droplet size decreases with increasing droplet charge density. This may be interpreted as the facilitation of droplets rupture by electrical repulsion forces.

The basic phenomenon in electrostatic atomization is the jet, which is formed when an electric field pulls fluid away from the surface. The electrical force operating on the fluid comes from the free charge conducted to the jet surface by the electric field inside the jet. Atomization takes place when the jet is broken into drops by counteracting forces due to surface tension and free charge on the jet surface. Atomization rate increases as the voltage, i.e. the electric field at the atomizing surface is increased. However, the formation of the corona at the atomizing surface or edge limits the atomization rate.

An interesting phenomenon in the field of atomization is the effect that an applied electric field has on a liquid jet emanating from a capillary tube. Under the optimum conditions, namely with the optimum combination of rheological/electrical properties, voltage, flow rate and system geometry, the fluid forms a conical shape at the exit of the capillary. A fine jet emerges from the tip of this cone, resulting in droplets that are nearly uniform in size and are significantly smaller than the diameter of the capillary itself. This method of atomization shall be referred to as an “electrospray” or “cone-jet”.

The application of an electrostatic field to liquid emerging from a capillary tube provides a means for generating small droplets without the need for a small orifice and high pressure, as discovered experimentally by Zeleny (1915). The electric field generated in the capillary tube, the charged liquid and the ground electrode cause extensional forces in the liquid, resulting in a liquid cone and a thin jet at the tip of the cone. The potential gradient along the liquid jet generates a tangential electric field, acting on the surface charges. These surface forces stabilize the jet and enable Rayleigh break-up of the jet with generation of nearly monosize charged droplets, which migrate toward an electrically grounded counter-electrode plate. The formation of current driven jets was studied theoretically and experimentally by Taylor (1964), Melcher (1972), Hayati et al. (1987) and others. However, the application of electrosprays has not been studied extensively. Among the few works in this area, Tang and Gomez (1994) can be mentioned.

If the liquid mass flow rate is $\dot{M}_L$, the average charge-to-mass ratio of the droplet is approximately

$$\frac{q}{m} = \frac{I}{\dot{M}_L} \tag{1}$$

where I is the current in the voltage generator; however, this will not give any precise information for the individual droplet's charge-to-mass ratio.

Ganan-Calvo and Barrero (1999) studied the scaling laws for the cone-jet electrospray current and droplet size. They concluded that the average droplet charge reaches a maximum at approximately 80% of the Rayleigh limit [5-6]. Gemci et al. (2002) have identified the charge-to-mass ratio for a Rotary-Bell atomizer at high operating voltage rates of 40 and 70 kV. Their charge-to-mass ratio results for larger droplets in the range of 4 to 80 μm coincided with the boundary limit of the Paschen line.

Electrostatic Limitation On Drop Charge

There are limits to the amount of drop charge that can be retained on the droplet surface. Fundamentally two physical mechanisms limit the charge that can be carried by a drop. The Rayleigh limit describes a charge above which the inward stress due to surface tension cannot balance the outward stress due to the electric field that is terminated by the surface charge density (Melcher, 1981). A drop that is charged above the Rayleigh limit experiences electromechanical instability and disintegrates into at least two smaller drops. For a drop with diameter D, and with vacuum permittivity (ε_o) and surface tension (γ) at the spherical interface of the drop with the surrounding air, the Rayleigh limit on drop charge (q_R) and the corresponding charge-to-mass ratio at the Rayleigh limit for a drop with a mass (m) and density (ρ) are:

$$q_R = \pi\sqrt{8\varepsilon_o \gamma D^3} \quad \text{and} \quad \frac{q_R}{m} = \frac{12\sqrt{2}}{\rho}\sqrt{\frac{\varepsilon_o \gamma}{D^3}} \tag{2}$$

Localized electrical discharge due to avalanche ionisation processes (corona) can occur at the surface of a charged drop (Crowley, 1986 and Castle et al., 1991). For drops with diameters larger than 200 μm, corona discharge occurs when the electric field exceeds a value that is a weak function of drop radius and that is at least $3x10^6$ V/m, the "breakdown" value for air at standard temperature and pressure in a uniform electric field. For drops with diameters less than 200 μm, corona discharge requires a voltage at the surface of the drop of approximately V_P = 0.327 kV, a value necessary for ionising collisions. The charge that yields this latter condition is referred to as the Paschen limit (q_P) and has the value with the corresponding charge-to-mass ratio (q_P/m):

$$q_P = 2\pi\varepsilon_o D\, V_P \quad \text{and} \quad \frac{q_P}{m} = \frac{12\varepsilon_o V_P}{\rho D^2} \tag{3}$$

Experimental Setup and Results

In order to use the PDI system to measure charges on individual drops, we have devised simple means to accelerate the drops to terminal velocity in a known uniform electric field after they pass through a small hole in the deposition electrode, as portrayed in Figure 1. The cone-jet electrospray was generated through a capillary

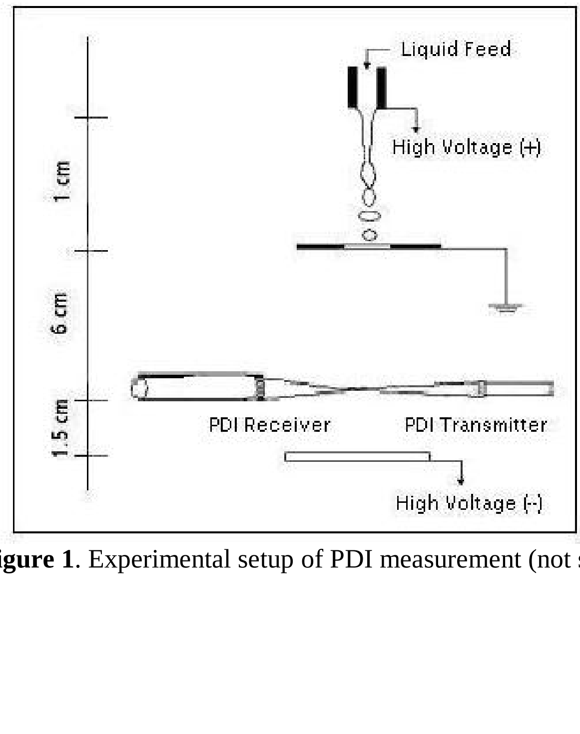

Figure 1. Experimental setup of PDI measurement (not scaled)

tube with an inside diameter of 180 μm and the propylene glycol was used as liquid with a flow rate of 1 μl/min. The PDI system is positioned 6 cm below the grounded ring electrode so as to measure sizes and velocities of individual drops as they pass through the applied uniform electric field region.

The balance of the electrical and gravitational forces with viscous drag in air at terminal velocity for a drop of known diameter can be expressed by the formula

$$ma = F_{total} = F_e + F_g + F_D \tag{4}$$

where F_e is the electrical force acting on a droplet, F_g and F_D are the gravity and drag forces. Equation (4) can be written with these terms when a droplet reaches its terminal velocity, i.e. without acceleration:

$$qE + mg - C_D \frac{\pi D^2}{4} \frac{\rho_{air} V^2}{2} = 0 \tag{5}$$

By measuring the droplet diameter (D) and droplet velocity (V) with Phase Doppler Interferometry in a known electric field (E), the charge on a droplet (q) can be determined with a calculation of the drag coefficient as a function of the droplet Reynolds number:

$$q = C_D(Re_d)\ \frac{\pi \rho_{air} D^2 V^2}{8E} - \frac{mg}{E} \tag{6}$$

The drag coefficients as a function of the droplet Reynolds number (Re_d) for the range between 0 and 400, which covers this experimental range, were calculated [15] as follows.

$$C_D = \begin{cases} 24 / Re_d & for \quad 0 < Re_d < 1 \\ 24 / Re_d^{0.646} & for \quad 1 < Re_d < 400 \end{cases} \tag{7}$$

Figure 2 shows the plot of the measured correlation between droplet size and velocity for the cone-jet electrospray at the operating voltage of 4.2 kV. Each point in this figure represents a single drop that passed through the beam intersection region. After a data set is collected by the PDI system, it can be efficiently processed to provide information that characterizes the mechanical and electrical properties of the spray. The PDI beams are positioned so as to cross far enough below the grounded washer electrode to assure that the drop has accelerated to its terminal velocity prior to the measurement of its diameter and velocity. The PDI system is capable of measuring and recording diameters and velocities (as shown in Figure 2) of thousands of individual drops in a period of 20 seconds. Most droplets are in the range between 2 and 5 μm having average velocities between 5 and 7 m/s. Increasing voltage from 4.2 kV to 4.8 kV causes a decrease in drop sizes (most sizes are between 1 and 3 μm) and also an increase in average velocities (between 6 and 10 m/s). By a further increase of applied voltage to 5.4 kV the droplets were detected as small as 0.5 μm, which is an instrumental limit based on the laser beam wavelength (see Figure 3). This figure also indicates a broadening of the velocity range for a given drop size as voltage is increased. The majority of droplets with an applied voltage of 5.4 kV have a terminal velocity that ranges from 4 to 9 m/s, compared to a range of 5 to 7 m/s for an electrospray with a 4.2 kV applied voltage.

The charge on each drop is calculated on the basis of a numerical solution of Equation (6), which balances electrical, gravitational and drag forces for measured droplets at the terminal velocity in the known uniform electric field (obtained from ANSYS package by simulating the electric field (E) between the capillary tube and electrode plates). The Reynolds number and drag coefficient for each droplet are obtained from Equation (7). The charge-to-mass ratio of each individual drop is then plotted, to yield Figures 4-6, the distribution of the charge-to-mass ratio versus drop diameter on a semi-log axes for the cone-jet electrospray with the operating voltages at 4.2, 4.8, and 5.4 kV, respectively. Also indicated in Figures 4-6 are lines that correspond to the Rayleigh limit associated with electromechanical instability and the Paschen limit associated with the breakdown field for air at the surface of a charged drop.

For drop sizes below approximately 5.5 μm the Rayleigh limit expresses the upper boundary of the charge-to-mass ratio. When the charge exceeds the Rayleigh limit, Coulumb repulsion overcomes surface tension leading to droplet disintegration. Beyond 5.5 μm the Paschen limit represents the upper boundary of the charge-to-mass ratio. The drop diameters for the cone jet are small enough to enter the regime for which the Rayleigh limit is lower than the Paschen limit. At the lowest charge voltage of 4.2 kV, Figure 4 shows that there is a gap between the Rayleigh boundary limit and the experimentally determined droplet charge-to-mass ratios.

Additionally Figure 4 shows a greater variability in the charge-to-mass ratio at a specific drop size due to electromechanical-hydrodynamic instabilities. As the diameters of the droplets decrease the variability in charge-to-mass ratio decreases; represented by the decrease in the width of the experimental data band. This experimental data band also appears to be constrained by a lower boundary condition. When the charging voltages are increased gradually, the droplet charge-to-mass ratio band approaches the Rayleigh limit and for the 4.8 and 5.4 kV cases the upper boundary of this band coincides with the Rayleigh line as seen in Figure 5 and Figure 6. Increasing the voltage causes an increase in the specific charge and also a decrease in the droplet size, which is a result of further electrohydrodynamic break-up processes when the droplets reach the maximum charge of the Rayleigh limit. Therefore the particle density in the 0.5 to 4 μm range is highest at an applied voltage of 5.4 kV.

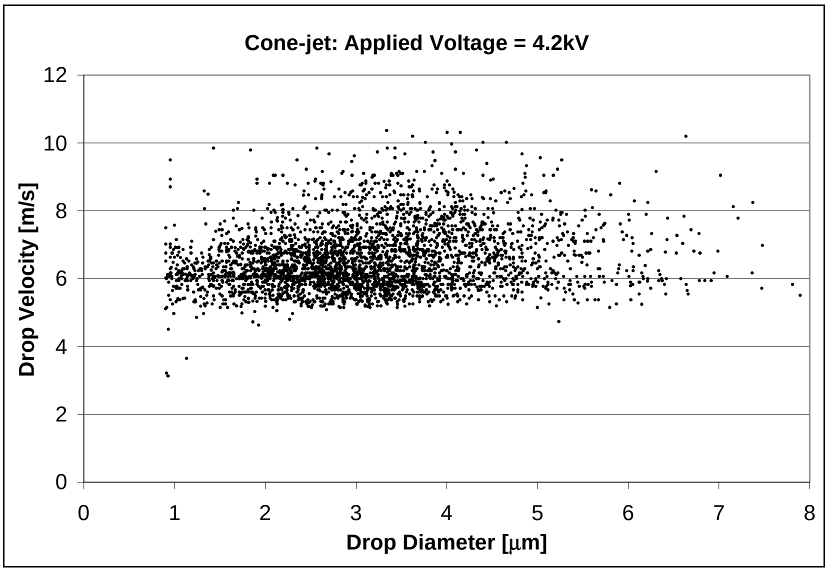

Figure 2. Measured correlation between drop diameters and velocities for the cone-jet at 4.2 kV

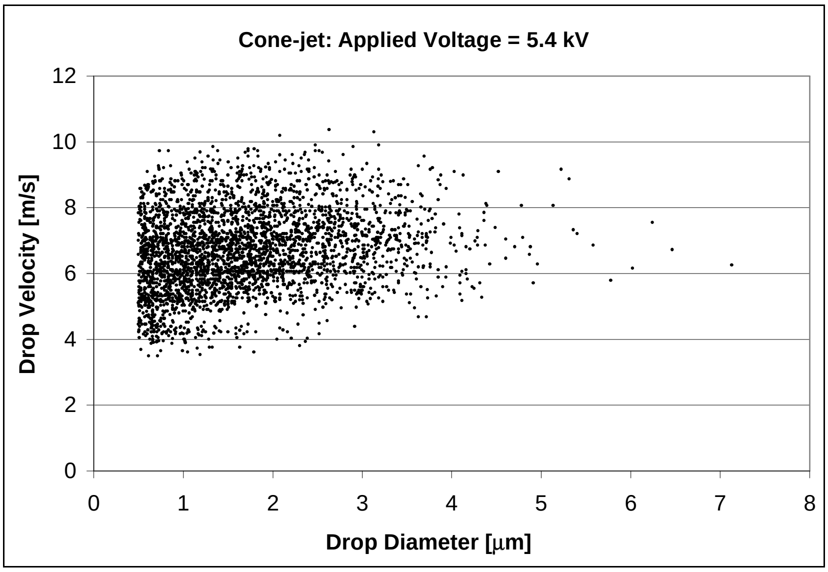

Figure 3. Measured correlation between drop diameters and velocities for the cone-jet at 5.4 kV

Conclusions

The distribution of charge-to-mass ratios for the cone-jet electrospray, based upon measurements of thousands of individual drops, is remarkably well correlated with the Rayleigh charge limiting theory. The upper limit of the experimental charge-to-mass ratio distribution coincides perfectly with the Rayleigh limit line. In summary, it has been shown that the PDI diagnostic method provides detailed and accurate data on drop size and charge distributions, which can be both gathered and processed efficiently. This method proved to be viable for electrostatic spray systems that span a range from large industrial devices to small-scale laboratory setups.

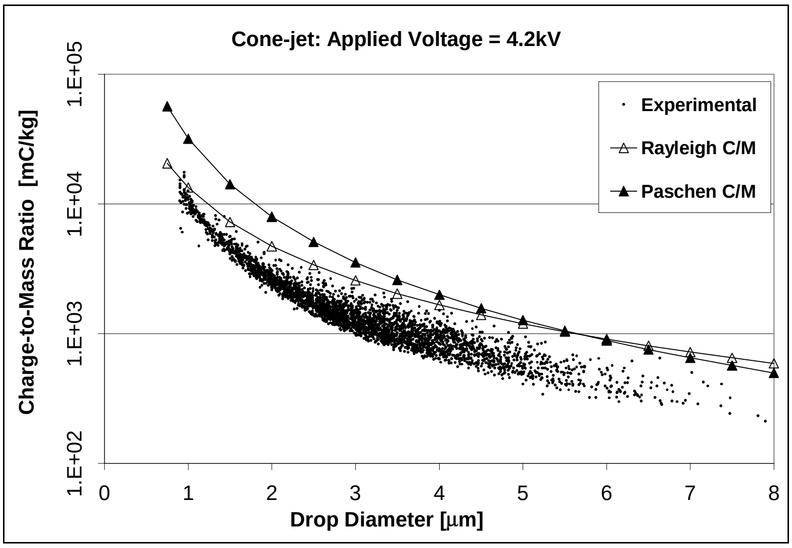

Figure 4. Charge-to-mass ratio vs. drop diameter for the cone-jet at 4.2 kV

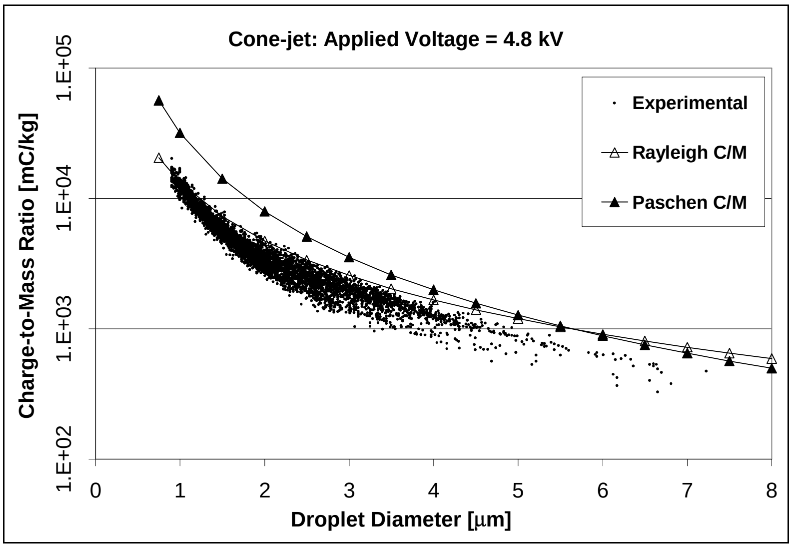

Figure 5. Charge-to-mass ratio vs. drop diameter for the cone-jet at 4.8 kV

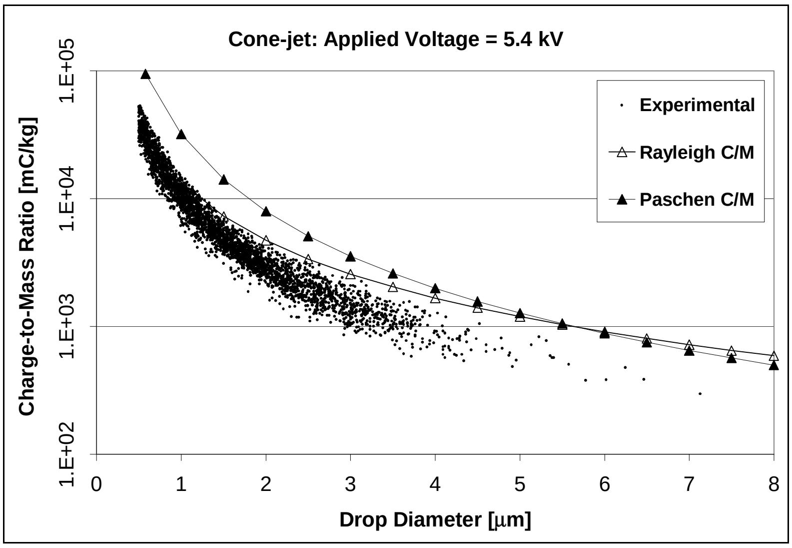

Figure 6. Charge-to-mass ratio vs. drop diameter for the cone-jet at 5.4 kV

Nomenclature

D	droplet diameter
a	acceleration
C_D	drag coefficient
E	electric field
F	force acting on a drop
I	current
g	gravity
m	droplet mass
q	charge on a drop
Re_d	droplet Reynolds number
V	droplet velocity
V_p	voltage
ρ	droplet density
ρ_{air}	air density
γ	surface tension
ε_o	vacuum permittivity

Subscripts

D	drag
d	drop
e	electric
g	gravity
P	Paschen limit
R	Rayleigh limit

References

[1] Brand, O. et al., “Microjet cooling devices for thermal management of microelectronics devices,” *IEEE Solid-State Sensor and Actuator Workshop*, Hilton Head Island, South Carolina, June 7-11, 1998.

[2] Cloupeau, M et al., “Electrostatic spraying of liquids: Main functioning modes,” *J. of Electrostatics*, 25, 165-184 (1990).

[3] Castle, G.S.P. and Inculet, I.I., “Induction charge limits of small water droplets,” *Electrostatics ’91*, Oxford, 1991, pp. 141-146.

[4] Crowley, J.M., *Fundamentals of Applied Electrostatics*, Wiley-InterScience, pp. 27-29, 1986.

[5] Pantano, C., Ganan-Calvo, A.M., and Barrero, A., “Zeroth-order electrohydrostatic solution for electrospraying in cone-jet mode,” *J. Aerosol Science*, 25(6): 1065-1077 (1994).

[6] Ganan-Calvo, A.M., Davila, J., and Barrero, A., “Current and droplet size in the electrospraying of liquids. Scaling laws,” *J. Aerosol Science*, 28(2): 249-275 (1997).

[7] Gemci, T, Hitron, R., and Chigier, N., “Measuring charge-to-mass ratio of individual droplets using Phase Doppler Interferometry,” *ILASS Americas 2002,* Madison, WI, May 14-17, 2002, pp. 241-245.

[8] Hayati, I., et al., “Investigations into the mechanisms of electrohydrodynamic spraying of liquids,” *J. of Colloid and Interface Science*, 117(1): 205-221 (1987).

[9] Jaworek, A., et al., “Forms of the multijet mode of electrohydrodynamic spraying,” *J. Aerosol Science*, 27:7, 979-986 (1996).

[10] Melcher, J.R., “*Continuum Electromechanics*,” MIT Press, Cambridge, MA, 1981, Sect. 8.13.

[11] Melcher, J.R., “Electrohydrodynamics,” *Proc. of the 13th international congress of theoretical and applied mechanics*, Moscow. pp. 240-263 (1972).

[12] Rulison, A.J. and Flagan, R.C., “Electrospray Atomization of Electrolytic Solutions,” *Journal of Colloid and Interface Science*, 167:135-145 (1994).

[13] Taylor, S G., “Disintegration of water drops in an electric field,” *Proc. Royal Society A* 280:383-397 (1964).

[14] Tang, K. and Gomez, A., “Generation by electrospray of monodisperse water droplets for targeted drug delivery by inhalation,” *J. Aerosol Science*, 25:6, 1237-1249 (1994).

[15] Zeleny, J., “On the conditions of instability of electrified drops, with applications to the electrical discharge from liquid points,” *Proc. of the Cambridge Philosophical Society*, 18:71-83 (1915).

[16] Zhang, Z., Kleinsteuer, C., and Kim, C.S., “Aerosol deposition efficiencies and upstream release positions for different inhalation models in an upper bronchial airway model,” *Aerosol Science and Technology,* 36(7): 803-856 (2002).